Mutational Analysis of the Substrate Specificity of *Escherichia coli* Penicillin Binding Protein 4[†]

Thomas B. Clarke,*[,‡,§] Fumihiro Kawai,[||] Sam-Yong Park,[||] Jeremy R. H. Tame,[||] Christopher G. Dowson,[‡] and David I. Roper*[,‡]

Department of Biological Sciences, University of Warwick, Gibbet Hill Road, Coventry CV4 7AL, U.K., and Protein Design Laboratory, Yokohama City University, Suehiro 1-7-29, Tsurumi-ku, Yokohama 230-0045, Japan

Received October 24, 2008; Revised Manuscript Received February 11, 2009

ABSTRACT: *Escherichia coli* PBP4 is the archetypal class C, low molecular mass penicillin binding protein (LMM-PBP) and possesses both DD-carboxypeptidase and DD-endopeptidase activity. In contrast to other classes of PBP, class C LMM-PBPs show high DD-carboxypeptidase activity and rapidly hydrolyze synthetic fragments of peptidoglycan. The recently solved X-ray crystal structures of three class C LMM-PBPs (*E. coli* PBP4, *Bacillus subtilis* PBP4a, and *Actinomadura* R39 DD-peptidase) have identified several residues that form a pocket in the active site unique to this class of PBP. The X-ray cocrystal structure of the *Actinomadura* R39 DD-peptidase with a cephalosporin bearing a peptidoglycan-mimetic side chain showed that residues of this pocket interact with the third position *meso*-2,6-diaminopimelic acid residue of the peptidoglycan stem peptide. Equivalent residues of *E. coli* PBP4 (Asp155, Phe160, Arg361, and Gln422) were mutated, and the effect on both DD-carboxypeptidase and DD-endopeptidase activities was determined. Using *N*-acetylmuramyl-L-alanyl-γ-D-glutamyl-*meso*-2,6-diaminopimelyl-D-alanyl-D-alanine as substrate, mutation of Asp155, Phe160, Arg361, and Gln422 to alanine reduced k_{cat}/K_m by 12.7-, 1.9-, 24.5-, and 13.8-fold, respectively. None of the k_{cat} values deviated significantly from wild-type PBP4. PBP4 DD-endopeptidase activity was also affected, with substitution of Asp155, Arg361, and Gln422 reducing specific activity by 22%, 56%, and 40%, respectively. This provides the first direct demonstration of the importance of residues forming a subsite to accommodate *meso*-2,6-diaminopimelic acid in both the DD-carboxypeptidase and DD-endopeptidase activities of a class C LMM-PBP.

The bacterial cell is surrounded by multiple layers of peptidoglycan, which are essential for viability (*1*). *Escherichia coli* peptidoglycan is a carbohydrate polymer of alternating *N*-acetylglucosamine and *N*-acetylmuramic acid residues. Appended to the D-lactyl group of *N*-acetylmuramic acid is a stem peptide, L-alanyl-γ-D-glutamyl-*meso*-2,6-diaminopimelyl-D-alanyl-D-alanine (*2*). In the mature peptidoglycan polymer, stem peptides are generally cross-linked directly between the third position *meso*-2,6-diaminopimelic acid and the fourth position D-alanine of an adjacent stem (*3*). Synthesis and remodeling of the peptidoglycan polymer are performed by the penicillin binding proteins (PBPs),[1] which are divided into two groups by molecular mass: high molecular mass (HMM) PBPs (>60 kDa) and low molecular mass (LMM) PBPs (<60 kDa) (*4, 5*). The HMM-PBPs synthesize nascent peptidoglycan, with polymerization of the carbohydrate backbone catalyzed by transglycosylases and cross-linking between stem peptides by transpeptidases (*4, 6*). LMM-PBPs have two main catalytic activities *in vivo*, DD-carboxypeptidation and DD-endopeptidation, and are split into three classes by sequence: A, B, and C (*7*). Class A enzymes are monofunctional DD-carboxypeptidases and are typified by *E. coli* PBP5 (*8*). Class B enzymes show sequence similarity to class C β-lactamases with *Streptomyces* R61 DD-peptidase being the best studied member of this class (*7, 9*). Class C enzymes are bifunctional, catalyzing both DD-carboxypeptidation and DD-endopeptidation (Figure 1), and show sequence similarity to class A β-lactamases (*7, 10*). LMM-PBPs are not essential for bacterial viability *under laboratory conditions*, and this has hindered attempts to define their function(s) *in vivo* (*11*); however, their ubiquity implies strong conservational pressure and an as yet undefined role in the bacterial life cycle.

E. coli has a complement of seven LMM-PBPs (PBP4, PBP5, PBP6, PBP7, DacD, AmpC, and AmpH) (*8, 12, 13*). PBP4 is the only class C LMM-PBP and is encoded by the *dacB* gene (*14*). The X-ray crystal structure of PBP4 showed that it is composed of three distinct domains, the majority of the structure being derived from domains I and II which

[†] This work was supported by a BBSRC Ph.D. studentship award to T.B.C. (BBSSC200412641) and in part by MRC Grants G0400848 and G500643.

* To whom correspondence should be addressed. D.I.R.: e-mail, david.roper@warwick.ac.uk; telephone, +44 24 7652 8369; fax, +44 24 7652 3701. T.B.C.: e-mail, clarket@mail.med.upenn.edu; telephone, (215) 573-3510; fax, (215) 573-4856.

[‡] University of Warwick.

[§] Present address: Department of Microbiology, University of Pennsylvania School of Medicine, Philadelphia, PA 19104.

[||] Yokohama City University.

[1] Abbreviations: PBP, penicillin binding protein; HMM, high molecular mass; LMM, low molecular mass; IDH, isocitrate dehydrogenase; PK, pyruvate kinase; MRW, mean residue weight; NAM, *N*-acetylmuramic acid; peptide **1**, *N*-acetylmuramyl-L-alanyl-γ-D-glutamyl-*meso*-2,6-diaminopimelyl-D-alanyl-D-alanine; peptide **2**, *N*-acetylmuramyl-L-alanyl-γ-D-glutamyl-L-lysyl-D-alanyl-D-alanine; peptide **3**, L-alanyl-γ-D-glutamyl-L-lysyl-D-alanyl-D-alanine.

10.1021/bi801993x CCC: $40.75
Published on Web 02/11/2009

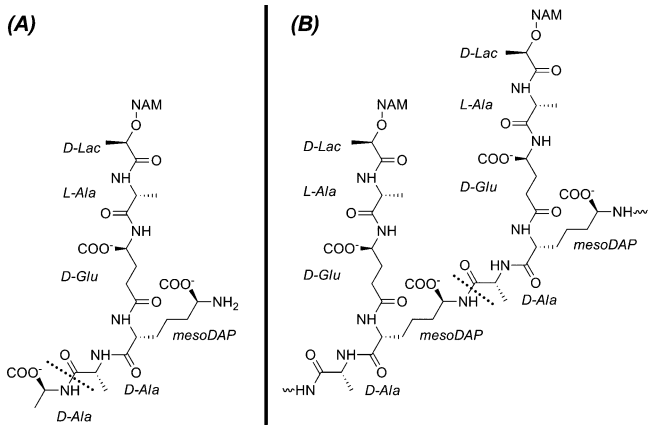

FIGURE 1: Bonds cleaved by the DD-carboxypeptidase and DD-endopeptidase activities of *E. coli* PBP4. (A) DD-Carboxypeptidation results in hydrolysis of the terminal peptide bond of the peptidoglycan stem peptide releasing the terminal D-alanine. (B) DD-Endopeptidase activity cleaves the cross-linking peptide bond between the fourth position D-alanine and third position *meso*-2,6-diaminopimelic acid of an adjacent stem peptide. Peptide bonds hydrolyzed by PBP4 are represented by a dashed line. NAM, *N*-acetylmuramic acid, *N*-acetylglucosamine residues, and bonds between adjacent sugars of the glycan backbone are omitted for clarity.

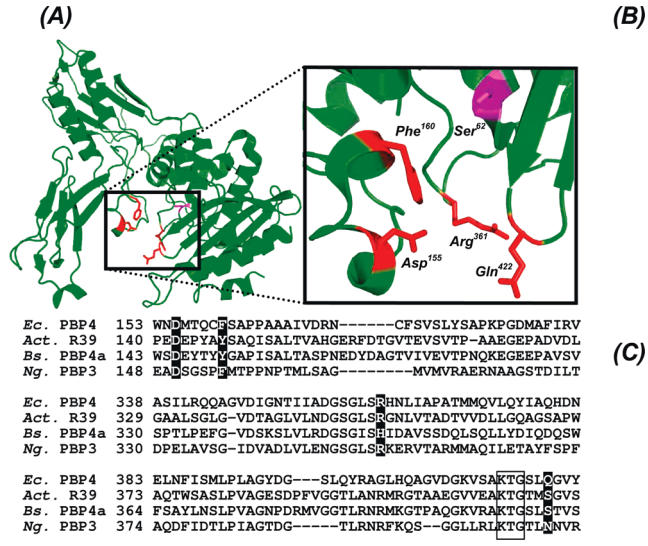

FIGURE 2: X-ray crystal structure of *E. coli* PBP4 highlighting residues forming a subsite within the active site important in substrate specificity. (A) Ribbon representation of the overall structure of PBP4 (PDB 2EX2). (B) Inset: Ribbon representation of the active site, highlighting residues that have been implicated in recognition of the stem peptide *meso*-2,6-diaminopimelic acid. The active site serine is shown in purple, and the residues forming a potential *meso*-2,6-diaminopimelic acid binding pocket in stick representation are colored red. (C) Sequence alignment of *E. coli* PBP4 (*Ec.* PBP4), *Actinomadura* R39 DD-peptidase (*Act.* R39), *B. subtilis* PBP4a (*Bs.* PBP4a), *Neisseria gonorrhoeae* PBP3 (*Ng.* PBP3) showing equivalent residues (shown white against black) in other characterized class C LMM-PBPs. PBP signature motifs essential for activity are boxed. Sequences were aligned using ClustalW.

are similar to domains I and II of *E. coli* PBP5 (*15, 16*). The active site serine (Ser62) is located in a groove created by β-sheet 1 of domain I and domain III that is approximately 20 Å deep and 15 Å wide, allowing access for peptidoglycan and/or β-lactams (Figure 2A). An interesting feature of the *E. coli* PBP4 structure is the presence of a subsite in the substrate pocket, similar structures being present in other class C LMM-PBPs (*Bacillus subtilis* PBP4a and *Actinomadura* R39 DD-peptidase) (*17, 18*). Amino acid side chains forming this subsite are thought to be involved in substrate specificity via recognition of the *meso*-2,6-diaminopimelic acid residue of the stem peptide. This hypothesis is supported by the recently solved X-ray crystal structure of *Actinomadura* R39 DD-peptidase in complex with a cephalosporin bearing a peptidoglycan-mimetic side chain. This model shows specific interactions between the ammonium−carboxylate group of *meso*-2,6-diaminopimelic acid and a subsite composed of Asp142, Tyr147, Arg351, and Ser415 (*Actinomadura* R39 numbering) (*19*).

Residues comprising the subsite are well conserved among the class C LMM-PBPs (Figure 2C), but their importance in enzyme activity is unclear due to differences in the kinetics of DD-carboxypeptidation catalyzed by this class of PBP. *Actinomadura* R39 DD-peptidase rapidly hydrolyzes the *meso*-2,6-diaminopimelic acid containing peptidoglycan-mimetic, D-α-aminopimelyl-ϵ-D-alanyl-D-alanine (k_{cat}/K_m = 5700 $mM^{-1}\cdot s^{-1}$) (*20*). The high specificity constant is due to a low K_m (K_m = 1.3 μM) suggesting that recognition of *meso*-2,6-diaminopimelic acid is key to its DD-carboxypeptidase activity. The kinetics of *N. gonorrhoeae* PBP3 DD-carboxypeptidase activity are also rapid (k_{cat}/K_m = 180 $mM^{-1}\cdot s^{-1}$, for the generic stem peptide N^{α}-Boc-N^{ϵ}-Cbz-L-lysyl-D-alanyl-D-alanine) (*21*). However, the high specificity constant is due to a high turnover number, not a low K_m (k_{cat} = 580 s^{-1}), implying that extended features of the stem peptide are not important for *N. gonorrhoeae* PBP3 DD-carboxypeptidase activity. *B. subtilis* PBP4a also hydrolyzes D-α-aminopimelyl-ϵ-D-alanyl-D-alanine; however, in contrast to *Actinomadura* R39 DD-peptidase, the K_m is greater than 1 mM (*17*).

The current structural data therefore point toward an important role for residues forming the subsite in the DD-carboxypeptidase substrate specificity of class C LMM-PBP, whereas the kinetic data present no clear pattern. Additionally, the importance of these residues in DD-endopeptidase activity is completely unknown. In this paper we study the enzymology of both the DD-carboxypeptidase and DD-endopeptidase activities of *E. coli* PBP4 and use site-directed mutagenesis to demonstrate unambiguously the relative importance of Asp155, Phe160, Arg361, and Gln422 in both activities.

MATERIALS AND METHODS

Chemical Reagents. All chemicals and reagents were purchased from Fisher Scientific (U.K.), Calbiochem (USA), and Sigma (USA) unless stated otherwise. Pig heart isocitrate dehydrogenase (IDH) and rabbit muscle pyruvate kinase (PK) were purchased from Sigma. Oligonucleotide primers were purchased from VHBio (U.K.).

Auxiliary Enzymes. Vectors carrying *Pseudomonas aeruginosa murB*, *murC*, *murD*, *murE*, and *murF* were a gift from Prof. R. C. Levesque (Université Laval). Vectors carrying *Streptococcus pneumoniae murE* and *murF* were a gift from Dr. A. M. Blewett (University of Warwick). A ligation-independent cloning kit (Novagen) was used to construct an expression vector carrying *S. pneumoniae murA-2* following the manufacturer's instructions, using the following primers: 5′-GAC GAC GAC AAG ATG GAT AAA ATT GTG GTT

Table 1: Oligonucleotide Primers Used To Create Site-Directed Mutants of *E. coli* PBP4[a]

primer	sequence (5′ → 3′)
F160A for	TGGAATGACATGACACAATGCGCTAGCGCTCCGCCTGCCGCCGCC
F160A rev	GGCGGCGGCAGGCGGAGCGCTAGCGCATTGTGTCATGTCATTCCA
D155A for	CCGGCTGGCCATGGAATGCCATGACACAATGCTTTAGCGCTC
D155A rev	GGAGCGCTAAAGCATTGTGTCATGGCATTCCATGGCCAGCCGG
R361A for	GCCGATGGTTCAGGGCTTTCGGCGCATAACCTGATTGCCCCCGCC
R361A rev	GGCGGGGGCAATCAGGTTATGCGCCGAAAGCCCTGAACCATCGGC
R361H for	GCCGATGGTTCAGGGCTTTCGCACCATAACCTGATTGCCCCCGCC
R361H rev	GGCGGGGGCAATCAGGTTATGTGCCGAAAGCCCTGAACCATCGGC
Q422A for	GTCTCAGCGAAAACCGGTTCGTTGGCGGGGGTATAACCTG
Q422A rev	CAGGTTATATACCCCCGCCAACGAACCGGTTTTCGCTGAGAC
Q422S for	GTCTCAGCGAAAACCGGTTCGTTGTCGGGGGGTATAACCTG
Q422S rev	CAGGTTATATACCCCCGACAACGAACCGGTTTTCGCTGAGAC

[a] pET21b::*dacB* was used as a template; mutated codons are underlined.

CAA GGT GGC-3′ and 5′-GAG GAG AAG CCC GGT TTA TTC ATC TTC ATC ACT TGC CTC-3′. Vectors carrying recombinant *murA-2* were verified by DNA sequencing. All DNA manipulations were performed using standard methodologies, and DNA samples were purified using QIAGEN plasmid miniprep kits. All recombinant Mur enzymes carried hexahistidine tags. For overexpression, 800 mL cultures of *E. coli* BL21(λDE3) harboring pET46::*murA-2* in Luria broth supplemented with 50 mg·mL^{-1} ampicillin were grown at 37 °C until an $A_{600} = 0.8$ was reached. MurA expression was induced with 1 mM isopropyl β-D-thiogalactopyranoside for 4 h at 25 °C. Culture pellets were lysed in 50 mM HEPES, pH 7.6, 50 mM NaCl, 2 mM $MgCl_2$, 0.2 mM PMSF 1 μM leupeptin, and 1 μM pepstatin, clarified by centrifugation at 50000*g* for 60 min at 4 °C, and subsequently fractionated by immobilized metal affinity chromatography on a nickel-Sepharose column equilibrated with lysis buffer. MurA eluted in lysis buffer + 0.5 M imidazole. All other Mur enzymes were purified using the same protocol.

Overexpression and Purification of E. coli PBP4. The *E. coli dacB* gene, amplified from *E. coli* K12 genomic DNA, was cloned into pET21b (pET21b::*dacB*) as described previously (*15*). For overexpression, 800 mL cultures of *E. coli* BL21(λDE3) harboring pET21b::*dacB* in Luria broth supplemented with 50 mg·mL^{-1} ampicillin were grown at 37 °C until an $A_{600} = 0.6$ was reached. PBP4 expression was induced with 0.5 mM isopropyl β-D-thiogalactopyranoside for 6 h at 20 °C. PBP4 was purified as described previously (*15*).

Site-Directed Mutagenesis of E. coli PBP4. The Stratagene QuikChange site-directed mutagenesis kit was used to introduce the desired amino acid substitutions within PBP4 following the manufacturer's instructions using *PfuTurbo* DNA polymerase. The corresponding oligonucleotide primer pairs are outlined in Table 1. Mutated plasmid DNA was sequenced and aligned with the wild-type gene sequence to check for incorporation of the desired mutation.

Preparation of Peptidoglycan Fragments. N-Acetylmuramyl-L-alanyl-γ-D-glutamyl-*meso*-2,6-diaminopimelyl-D-alanyl-D-alanine (peptide **1**) and *N*-acetylmuramyl-L-alanyl-γ-D-glutamyl-L-lysyl-D-alanyl-D-alanine (peptide **2**) were produced by mild acid hydrolysis of UDP-*N*-acetylmuramyl-L-alanyl-γ-D-glutamyl-*meso*-2,6-diaminopimelyl-D-alanyl-D-alanine and UDP-*N*-acetylmuramyl-L-alanyl-γ-D-glutamyl-L-lysyl-D-alanyl-D-alanine, the synthesis of which is outlined in refs *22* and *23*. A modified version is given here; a typical 2 mL reaction composed of 50 mM HEPES, pH 7.5, 10 mM $MgCl_2$, 50 mM KCl, 10 mM DTT, 10 mM UDP-GlcNAc, 30 mM L-alanine, 30 mM D-glutamate, 30 mM *meso*-2,6-diaminopimelic acid, 30 mM D-alanyl-D-alanine, 200 mM phosphoenolpyruvate, 200 μM NADPH, 6 mM ATP, 25 mM isocitrate, 40 units of IDH, 500 units of PK, 300 μg of *S. pneumoniae* MurA, 2000 μg of *P. aeruginosa* MurB, 750 μg of *P. aeruginosa* MurC, 1000 μg of *P. aeruginosa* MurD, 1250 μg of *P. aeruginosa* MurE, and 1500 μg of *P. aeruginosa* MurF was incubated overnight at 37 °C and then purified by anion-exchange chromatography using Source 30Q resin. UDP-*N*-acetylmuramyl-pentapeptide with L-lysine at position 3 was produced using exactly the same protocol; however, *meso*-2,6-diaminopimelic acid was replaced with L-lysine and *P. aeruginosa* MurF and MurE were replaced by *S. pneumoniae* MurE and MurF. Electrospray ionization mass spectrometry (negative ion) was used to confirm the molecular weight of synthesized UDP-*N*-acetylmuramyl-peptides. Purity was assessed by analytical anion-exchange chromatography using a Mono Q HR5/5 column. *N*-Acetylmuramyl-peptides were produced by mild acid hydrolysis (0.1 M HCl, 100 °C, 1 h) of the corresponding UDP-*N*-acetylmuramyl-peptides. Peptides were subsequently analyzed by electrospray ionization mass spectrometry (positive ion). The concentration of other hydrolysis products (UDP, UMP, and P_i) was established by continuous spectrophotometric enzyme assay. Corresponding concentrations of UDP, UMP, and P_i were used in control spectrophotometric assays for D-alanine release to ensure they did not interfere with either PBP4 or coupling enzyme activity. L-Alanyl-γ-D-glutamyl-L-lysyl-D-alanyl-D-alanine (peptide **3**) was purchased from Sigma.

Continuous Spectrophotometric Assay for E. coli PBP4 DD-Carboxypeptidase Activity. DD-Carboxypeptidase activity was followed by a continuous spectrophotometric assay measuring D-alanine release, modified from ref *24*, on a Varian Cary 100 spectrophotometer at 37 °C. Briefly, D-amino acid oxidase catalyzes the oxidative deamination of D-alanine to pyruvate and hydrogen peroxide. The resulting hydrogen peroxide is reduced to H_2O by horseradish peroxidase, using Amplex Red (Molecular Probes, U.K.) as an electron donor. Oxidation of Amplex Red generates resorufin which has an intense spectrophotometric peak at 563 nm ($\epsilon_{563nm} = 53000$ M^{-1}·cm^{-1}). A typical assay had a final volume of 200 μL and was composed of 50 mM HEPES, pH 7.6, 10 mM $MgCl_2$, 3 units of D-amino acid oxidase, and 6 units of horseradish peroxidase. The final concentration of PBP4 and peptidoglycan substrate is stated in the text.

Isolation of Insoluble E. coli Peptidoglycan. Insoluble *E. coli* peptidoglycan was isolated from *E. coli* JM109, an *E.*

coli K12 derivative, using a protocol modified from ref *25*. Four liters of midlog phase *E. coli* JM109 was harvested by centrifugation. The pellet was washed with dH_2O and boiled in 4% (w/v) SDS for 30 min. The boiled culture was centrifuged at 70000*g* and the pellet washed three times with dH_2O. The pellet was resuspended in Tris·HCl, pH 7.6, + 50 $\mu g \cdot mL^{-1}$ DNase, + 100 $\mu g \cdot mL^{-1}$ RNase, incubated for 1 h at 37 °C, and harvested by centrifugation at 70000*g*. The pellet was washed three times with dH_2O, sonicated, and resuspended in 10 mM HEPES, pH 7.6, + 30 $\mu g \cdot mL^{-1}$ trypsin. After digestion with trypsin, the peptidoglycan preparation was washed three times with dH_2O and lyophilized. Approximately 8 mg of insoluble peptidoglycan was isolated per liter of culture.

Zymogram Analysis of E. coli PBP4 DD*-Endopeptidase Activity.* Zymogram analysis was performed using 12% (w/v) SDS−PAGE gels containing 0.1% (w/v) insoluble *E. coli* peptidoglycan and 0.01% (w/v) SDS. After electrophoresis the zymogram gels were washed twice in dH_2O for 10 min at 25 °C, then transferred to a renaturing buffer (25 mM Tris·HCl, pH 8.0, 0.1% (v/v) Triton X-100, and 10 mM $MgCl_2$), and incubated for 12 h at 37 °C to facilitate protein refolding. DD-Endopeptidase activity results in the hydrolysis of insoluble peptidoglycan visualized by staining with 0.1% (w/v) methylene blue and 0.01% (w/v) KOH and seen as a zone of clearing against a dark background.

Turbidometric Assay for E. coli PBP4 DD*-Endopeptidase Activity.* DD-Endopeptidase activity was monitored using a turbidometric assay based on the solubilization of insoluble *E. coli* peptidoglycan (*26*). Hydrolysis of insoluble peptidoglycan results in a reduction of A_{600}. Purified peptidoglycan was resuspended in 50 mM HEPES, pH 7.6, 10 mM $MgCl_2$, and 1 mM DTT and sonicated briefly to homogenize the suspension. Peptidoglycan concentrations below 0.2 $mg \cdot mL^{-1}$ could not be used, as the A_{600} was low and inconsistent; 1 $mg \cdot mL^{-1}$ was used as it gave the most reproducible A_{600}. Two micrograms of purified PBP4 was added to the insoluble peptidoglycan suspension, and the subsequent decrease in turbidity was monitored at 600 nm for 2 h at 37 °C. One unit of DD-endopeptidase activity was defined as the amount of enzyme required to reduce the A_{600} by 0.001 min^{-1} (*27*).

Circular Dichroism of Wild-Type and Mutant E. coli PBP4. Far-UV circular dichroism spectra were recorded on a Jasco J-715 spectropolarimeter using a 1 mm path-length quartz cuvette. All protein samples were at a final concentration of 1 μM in 20 mM sodium phosphate, pH 7.6, and 5 mM Na_2SO_4. Measurements were made in continuous scanning mode at a scanning speed of 100 $nm \cdot min^{-1}$ with a time constant of 1 s and bandwidth of 2 nm at 25 °C. For each spectrum the resolution was set to 0.5 nm, and eight scans were averaged. Corresponding buffer backgrounds were subtracted from the protein spectra.

$$[\theta]_{MRW} = \frac{\theta}{Ncl} \quad (1)$$

where θ = observed ellipticity (millidegrees), N = number of peptide bonds in the protein, c = molar protein concentration, and l = cuvette path length (cm). All of the mutants showed far-UV CD spectra very similar to that of the wild-type enzyme (Supporting Information Figure S1), indicating mutagenesis had not disrupted the structure of PBP4.

Analysis of Kinetic Data. Kinetic constants (K_m and k_{cat}) for DD-carboxypeptidation were determined by fitting data (initial velocities of PBP4 DD-carboxypeptidase activity versus substrate concentrations) to eq 2 by nonlinear regression using GraphPad Prism 4 software.

$$V_0 = \frac{V_{max}[S]}{K_m + [S]} \quad (2)$$

RESULTS AND DISCUSSION

Kinetic Parameters of E. coli PBP4 DD*-Carboxypeptidase Activity.* In comparison to other classes of PBP, all currently characterized class C LMM-PBPs display higher DD-carboxypeptidase activity (*28*). To establish the rate of PBP4 DD-carboxypeptidase activity, a continuous spectrophotometric assay for D-alanine release was used to determine k_{cat} and K_m with a variety of peptidoglycan fragments. Previous studies of the DD-carboxypeptidase activities of other PBPs have used generic tripeptide or tripeptide peptidoglycan-mimetic substrates (*20, 21, 28, 29*). The substrates used in this study were *N*-acetylmuramyl-pentapeptides, the type of peptidoglycan substrates PBP4 is likely to act upon *in vivo*. These were produced by mild acid hydrolysis of UDP-*N*-acetylmuramyl-pentapeptides to remove the attached UDP moiety. UDP-*N*-acetylmuramyl-pentapeptides were synthesized by *in vitro* reconstruction of the cytoplasmic steps in peptidoglycan biosynthesis. A potential problem with using these substrates was the presence of hydrolysis products (UDP, UMP, and P_i) in substrate preparations; therefore, a variety of control reactions were required to ensure that these products did not interfere with either PBP4 or coupling enzyme activity. DD-Carboxypeptidase activity was detected using the generic stem peptide, peptide **3**, as a substrate. This commercially available peptide does not contain contaminating UDP, UMP, or P_i and was used to control for the effect of these hydrolysis products. The rates of PBP4-catalyzed DD-carboxypeptidation using peptide **3** with and without the addition of UDP, UMP, and P_i at concentrations comparable to those of the *N*-acetylmuramyl-pentapeptide substrate preparations were identical (data not shown). Demonstrating that neither PBP4 nor the coupling enzymes horseradish peroxidase and D-amino acid oxidase were affected by the presence of the hydrolysis products and the observed rates may be considered a true reflection of PBP4-catalyzed DD-carboxypeptidation. As a further precaution, all steady-state kinetic assays for DD-carboxypeptidase activity were conducted in dual beam format with the assay initiated by the addition of substrate and in the reference cuvette by the addition of a control solution containing the equivalent concentration of UDP, UMP, and P_i to that of the substrate preparation. All substrates displayed a hyperbolic relationship between initial enzyme velocity (V_0) and substrate concentration (Figure 3) and were therefore fitted to the Michaelis−Menten equation (eq 2) to determine k_{cat} and K_m by nonlinear regression.

No reaction was detected using the terminal D-alanyl-D-alanine of the stem peptide as a substrate (data not shown), suggesting that recognition of additional elements of the peptidoglycan structure is required for catalysis. This is consistent with previous isothermal titration calorimetry data that failed to detect any binding of D-alanyl-D-alanine to

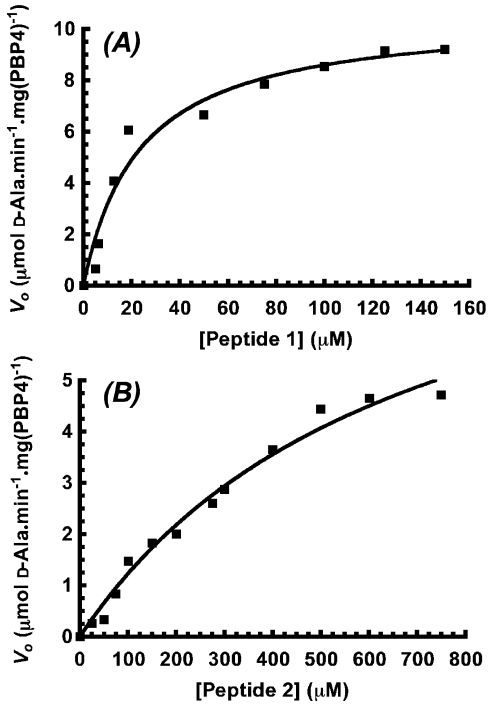

FIGURE 3: Kinetics of the dependence of *E. coli* PBP4 DD-carboxypeptidase activity on *N*-acetylmuramyl-pentapeptide substrate concentration. Initial velocity of *E. coli* PBP4-dependent D-alanine release (V_0) plotted versus *N*-acetylmuramyl-pentapeptide concentration. (A) V_0 plotted versus [peptide **1**] (μM); (B) V_0 plotted versus [peptide **2**] (μM). The final concentration of PBP4 in both (A) and (B) was 51 nM. Data were fitted to eq 2 by nonlinear regression.

PBP4 (*15*). Peptide **3** was a substrate for *E. coli* PBP4 with a $k_{cat}/K_m = 3.28$ mM^{-1}·s^{-1}, comparable to peptide **2** ($k_{cat}/K_m = 4.59$ mM^{-1}·s^{-1}), but only modest compared to peptide **1**. PBP4 showed highest DD-carboxypeptidase activity with peptide **1** ($k_{cat}/K_m = 170$ mM^{-1}·s^{-1}), 37-fold higher than with peptide **2** (Figure 3 and Table 2). The structure of these two peptidoglycan fragments is identical except for the third position amino acid of the stem peptide. The *meso*-2,6-diaminopimelic acid residue contains an additional carboxylate group on the ϵ-carbon atom, to which the ϵ-ammonium group of the third position L-lysine is also attached (Figure 1A). The difference in the rate of DD-carboxypeptidation between peptide **1** and peptide **2** must, therefore, be due to specific interactions between the *meso*-2,6-diaminopimelic acid ϵ-carboxylate and PBP4.

The presence of the *N*-acetylglucosamine and the D-lactate sugar residue of the stem peptide had only a minimal effect on DD-carboxypeptidase activity, increasing k_{cat}/K_m 1.4-fold. All substrates used had a complete pentapeptide stem, and hence the importance of the L-alanine and D-glutamate residues in substrate specificity was not addressed. The kinetic data for other PBPs suggest the importance of these residues is minimal (*20*), and furthermore there is no structural evidence demonstrating any interactions between these residues and any class of PBP (*4, 17, 18*).

Effect of Site-Directed Mutagenesis of Asp155, Phe160, Arg361, and Gln422 on DD-Carboxypeptidation. The substrate specificity displayed by PBP4 led us to investigate which residues were playing a role in mediating this preference. The structural similarity of PBP4 and *Actinomadura* R39 DD-peptidase suggested that residues in the PBP4 active site subsite may be important. The subsite in PBP4 is formed by residues from both domain I (Arg361 and Gln422) and domain II (Asp155 and Phe160) (Figure 2). The active site serine (Ser62) is situated in a readily accessible open groove approximately 20 Å deep and 15 Å wide, and the residues of the subsite form a crescent with their functional groups positioned approximately 10−15 Å from Ser62, ideally situated to interact with the third residue of the stem peptide. The X-ray crystal structure of *Actinomadura* R39 DD-peptidase in complex with cephalosporin bearing a peptidoglycan-mimetic side chain, specifically containing a *meso*-2,6-diaminopimelic acid, revealed further details about residues forming a subsite to accommodate the ammonium−carboxylate terminus of *meso*-2,6-diaminopimelic acid. The β-hydroxyl group of Ser415 and the guanidinium group of Arg351 are 3.1 and 2.7 Å away from the ϵ-carboxylate group of *meso*-2,6-diaminopimelic acid, respectively. Asp142 is situated opposite Ser415 and is 2.5 Å from the nitrogen of the *meso*-2,6-diaminopimelic acid ϵ-ammonium group (*18*). The three methylene groups are sandwiched between Tyr147 and Met414, a similar hydrophobic tunnel also being present in *E. coli* PBP4. To investigate if the equivalent residues in the *E. coli* PBP4 active site (Figure 2) are important in PBP4 DD-carboxypeptidase activity, Asp155, Phe160, Arg361, and Gln422 were all individually mutated to alanine (Table 2).

All recombinant mutant proteins were expressed and purified using the same protocol as the wild-type enzyme. The protein yields were similar to that of the wild-type enzyme, except for Asp155Ala and Phe160Ala, which expressed to approximately 60% and 75% of the wild-type level, respectively. Of the residues in the peptidoglycan binding subsite we mutated, replacement of Asp155, Arg361, or Gln422 with alanine had the greatest effect on the rate of DD-carboxypeptidation (Table 2). These reductions in the specificity constant of PBP4 show that these residues do play a role in DD-carboxypeptidase substrate specificity.

To define more precisely the roles of the individual residues in the subsite, we measured the kinetics of DD-carboxypeptidation catalyzed by mutant enzymes using peptide **2** as a substrate. The DD-carboxypeptidase activity of the Arg361Ala and Gln422Ala mutants of PBP4 with this substrate was very different from the results with *meso*-2,6-diaminopimelic acid at position 3 of the stem peptide. The loss of the guanidinium group of Arg361, or the loss of the Gln422 amide group, had a much smaller effect on catalysis with L-lysine at position 3 (Arg361Ala $k_{cat}/K_m = 3.86$ mM^{-1}·s^{-1} and Gln422Ala $k_{cat}/K_m = 4.69$ mM^{-1}·s^{-1}; wild-type $k_{cat}/K_m = 4.59$ mM^{-1}·s^{-1}). This strongly indicates that both Arg361 and Gln422 interact with the ϵ-carboxylate group of *meso*-2,6-diaminopimelic acid. A salt bridge is formed between Arg351 of the *Actinomadura* R39 DD-peptidase active site subsite and the ϵ-carboxylate group of *meso*-2,6-diaminopimelic acid, with a hydrogen bond also formed with Ser415 (*18*), and therefore it is probable that Arg361 and Gln422 perform these respective roles in PBP4. The Asp155Ala mutant showed a similar reduction in k_{cat}/K_m for both peptide **1** and peptide **2**, 12.7-fold and 9-fold, respectively. This similar reduction for both substrates implies that Asp155 interacts with the ϵ-ammonium group, a group present on both *meso*-2,6-diaminopimelic acid and L-lysine containing substrates. This concurs with structural

Table 2: Kinetics of Wild-Type and Mutant *E. coli* PBP4 DD-Carboxypeptidase Activity[a]

	substrate							
	peptide 1				peptide 2			
enzyme	K_m (μM)	k_{cat} (s^{-1})	k_{cat}/K_m ($mM^{-1}\cdot s^{-1}$)	activity decrease (*x*-fold)	K_m (μM)	k_{cat} (s^{-1})	k_{cat}/K_m ($mM^{-1}\cdot s^{-1}$)	activity decrease (*x*-fold)
WT	20.4 ± 1.65	3.47 ± 0.55	170		682 ± 122	3.13 ± 0.47	4.59	
D155A	222 ± 30.4	2.98 ± 0.49	13.4	12.7			0.51	9.0
F160A	34.4 ± 7.5	3.01 ± 0.51	87.5	1.9	913 ± 177	2.51 ± 0.34	2.75	1.7
R361A	401 ± 40.9	2.78 ± 0.21	6.93	24.5	744 ± 171	2.87 ± 0.59	3.86	1.2
R361H	178 ± 22.8	2.42 ± 0.35	16.4	10.4	712 ± 125	2.68 ± 0.26	3.76	1.2
Q422A	237 ± 31.5	2.91 ± 0.36	12.3	13.8	678 ± 103	3.18 ± 0.53	4.69	1.0
Q422S	116 ± 15.4	2.97 ± 0.5	25.6	6.6	675 ± 86	3.02 ± 0.48	4.47	1.0

[a] All kinetic constants were calculated using data obtained with 51 nM *E. coli* PBP4, except for the characterization of F160A, R361A, R361H, Q422A, and Q422S with peptide **2**, R361A and Q422A with peptide **1**, and D155A with either substrate, where 158 nM was used. All kinetic constants were determined according to eq 2 (±standard errors). Data were fitted to eq 2 by nonlinear regression.

data which shows the ϵ-ammonium group hydrogen bonding with Asp142 (equivalent to Asp155 of PBP4) of *Actinomadura* R39 DD-peptidase.

The nonpolar methylene chain of *meso*-2,6-diaminopimelic acid fits into a hydrophobic tunnel formed in part by Tyr147 in the *Actinomadura* R39 cocrystal structure (*18*). Since Phe160 is found in the equivalent position in *E. coli* PBP4, it might be expected to improve binding of the substrate, but mutation of this residue to alanine had only a marginal effect on catalysis (Phe160Ala $k_{cat}/K_m = 87.5$ $mM^{-1}\cdot s^{-1}$). The phenylalanine side chain appears to form only limited interactions with peptidoglycan, whose interactions with PBP4 through the *meso*-2,6-diaminopimelic acid residue are dominated by Asp155, Gln422, and Arg361.

Further mutations were made to investigate the roles of specific functional groups in the *meso*-2,6-diaminopimelic acid subsite (Table 2). *B. subtilis* PBP4a has a histidine residue (His352, *B. subtilis* numbering) in the equivalent position to Arg361 of *E. coli* PBP4 (Figure 2C). Substitution of Arg361 to histidine in *E. coli* PBP4 reduced k_{cat}/K_m 10.4-fold, a smaller reduction in comparison to the corresponding alanine substitution. The basic properties of the histidine imidazole ring thus partially compensate for the loss of the arginine guanidinium group. *Actinomadura* R39 DD-peptidase and *B. subtilis* PBP4a both have a serine in the equivalent position to the *E. coli* PBP4 Gln422 (Figure 2C). Replacement of Gln422 with serine results in $k_{cat}/K_m = 25.6$ $mM^{-1}\cdot s^{-1}$, a 6.6-fold change, but k_{cat}/K_m increased only marginally compared to Gln422Ala. These results can be explained if the β-hydroxyl group of serine forms a hydrogen bond with the ϵ-carboxylate group of *meso*-2,6-diaminopimelic acid, but weaker than the one formed by Gln422.

Effect of Site-Directed Mutagenesis of Asp155, Phe160, Arg361, and Gln422 on DD-Endopeptidation. In vivo it has been shown that *E. coli* PBP4 is a DD-endopeptidase, cleaving the cross-linking peptide bond between the fourth position D-alanine and third position *meso*-2,6-diaminopimelic acid of an adjacent stem peptide (*10*). Furthermore, it is thought that *in vivo* the predominant role of PBP4 is as a DD-endopeptidase (*8*), so we therefore wanted to know if the residues of the subsite play a role in DD-endopeptidation. PBP4 can perform both the DD-carboxypeptidase and DD-endopeptidase reactions due to the structural equivalence of the core element of the substrates. Specifically, the ϵ-carbon atom of *meso*-2,6-diaminopimelic acid cross-linked to an adjacent D-alanine is in the D-configuration and is equivalent to the penultimate D-alanine of the stem peptide. It is

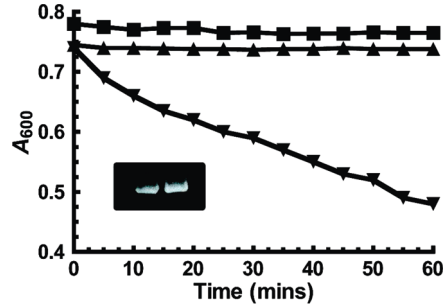

FIGURE 4: Turbidometric assay for E. *coli* PBP4 DD-endopeptidase activity. The decrease in turbidity at A_{600} of insoluble *E. coli* peptidoglycan (1 $mg\cdot mL^{-1}$) in 50 mM HEPES, pH 7.6, 10 mM $MgCl_2$, and 1 mM DTT was monitored with respect to time after the addition of wild-type PBP4. Wild-type PBP4 (▼), heat-inactivated PBP4 (▲), and BSA (■) were at a final concentration of 2 $\mu g\cdot mL^{-1}$. To avoid overlap, the time course of A_{600} change for BSA (■) has been shifted up 0.04 absorbance unit. Inset: Zymogram analysis of purified PBP4 using a 12% (w/v) SDS−PAGE gel containing 0.1% (w/v) insoluble *E. coli* peptidoglycan as substrate. DD-Endopeptidase activity was seen as a zone of clearing against a dark background after staining with 0.1% (w/v) methylene blue and 0.01% (w/v) KOH. Duplicate lanes are shown.

therefore proposed that PBP4, in DD-endopeptidation, positions the cross-linked *meso*-2,6-diaminopimelic acid in the active site as it would the penultimate D-alanine in DD-carboxypeptidation. To detect PBP4 DD-endopeptidase activity *in vitro*, a zymogram and turbidometric assay were performed with insoluble *E. coli* peptidoglycan as the substrate. Zymogram analysis showed that PBP4 hydrolyzed insoluble *E. coli* peptidoglycan (Figure 4 inset); this was confirmed by a turbidometric assay, which showed a decrease in A_{600} dependent on PBP4 (Figure 4). Based on the definition of murein hydrolase activity in ref *27*, 1 unit of DD-endopeptidase activity is the amount of enzyme required to decrease the A_{600} of the insoluble peptidoglycan preparation by 0.001 min^{-1}. The activity of wild-type PBP4 was 1785 $units\cdot mg^{-1}$; in comparison, hen egg white lysozyme was 4920 $units\cdot mg^{-1}$. Further turbidometric assays were conducted to gain quantitative data on the effect of mutation of Asp155, Phe160, Arg361, and Gln422 to alanine on PBP4 DD-endopeptidase activity (Table 3).

As with DD-carboxypeptidation, mutation of either Arg361 or Gln422 to alanine affected DD-endopeptidation, reducing specific activity by 56% and 40%, respectively. Mutation of Asp155 to alanine also had an effect on DD-endopeptidase activity but to a lesser extent, reducing specific activity by 22%. The free ϵ-ammonium group is lost in the mature peptidoglycan polymer as it forms the peptide bond with the

Table 3: DD-Endopeptidase Activity of Wild-Type and *E. coli* PBP4 Mutants[a]

enzyme	specific activity (units·(mg of PBP4)$^{-1}$)	relative specific activity (%) (compared to wild-type *E. coli* PBP4)
WT	1785 ± 268	
D155A	1231 ± 212	78
F160A	1624 ± 134	91
R361A	785 ± 180	44
Q422A	946 ± 149	60

[a] One unit of activity is defined as the amount of enzyme required to reduce A_{600} by 0.001 min^{-1}. Assays were performed with alanine mutants in triplicate at 37 °C (±standard errors).

fourth position D-alanine of the adjacent stem peptide. The small effect of the Asp155 to alanine mutation on DD-endopeptidase activity may reflect a change in the hydrogen bonds formed between PBP4 and the polymeric substrate compared to the hydrogen bonding with the monomeric substrate in DD-carboxypeptidation.

CONCLUSION

Penicillin binding protein substrate specificity is a topic of great debate due to the recalcitrance of these enzymes to catalyze *in vitro* the reactions that they readily perform *in vivo* (*30*). We recently solved the X-ray crystal structure of *E. coli* PBP4 (*15*) and present data here to further our biochemical characterization of this enzyme by (i) showing *E. coli* PBP4 has high DD-carboxypeptidase activity and demonstrates substrate specificity, (ii) addressing the individual role of Asp155, Phe160, Arg361, and Gln422 in DD-carboxypeptidase substrate specificity, and (iii) establishing that these residues are also involved in DD-endopeptidation.

Currently, only two PBPs (*Actinomadura* R39 DD-peptidase and *Streptomyces* R61 DD-peptidase) display any specificity for extended features of peptidoglycan (*20, 31*); however, the role of these enzymes *in vivo* is not understood, and therefore the relevance of their *in vitro* substrate specificity is unclear. The poor reactivity of most classes of penicillin binding protein is thought, in part, to be due to a failure to recognize extended features of peptidoglycan (*28*). Inspection of the X-ray crystal structure of *E. coli* PBP4 revealed a subsite in the active site not present in the X-ray crystal structures of any other class (HMM or LMM) of PBP (*15*). Similar structures were however present in other class C LMM-PBPs; furthermore, the *Actinomadura* R39 DD-peptidase has been cocrystallized with a cephalosporin bearing a peptidoglycan-mimetic side chain (Figure 5) and also a peptidoglycan-mimetic peptide, which show specific interactions between the subsite and the ammonium−carboxylate of the *meso*-2,6-diaminopimelic acid residue (*19*).

Additionally, the X-ray crystal structure of *Streptomyces* R61 DD-peptidase, a class B LMM-PBP, complexed with a peptidoglycan-mimetic revealed the presence of a substrate binding pocket with a structure different from those found in the class C enzymes, but thought to play a similar role in substrate specificity (*32*). *E. coli* PBP4 is the archetypal class C LMM-PBP, but to date it has remained only poorly functionally characterized. We have shown that PBP4 has a low K_m (K_m = 20.4 μM using peptide **1** as a substrate) which contrasts strongly with *E. coli* PBP5, the predominant DD-carboxypeptidase in *E. coli*, which has a K_m over 1 mM for

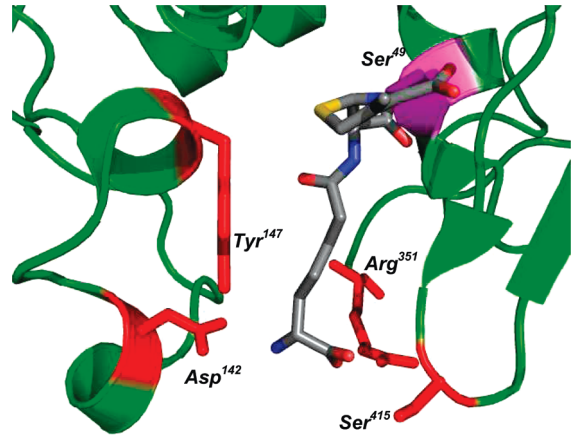

FIGURE 5: X-ray crystal structure of *Actinomadura* R39 DD-peptidase in complex with a modified cephalosporin bearing a peptidoglycan-mimetic side chain. Ribbon representation of the active site subsite; residues forming potential hydrogen bonds with the modified cephalosporin are labeled (*Actinomadura* R39 numbering). Side chains are shown in stick representation; nitrogens are shown in blue, oxygens are in red, and sulfur is in orange (PDB 2VGJ).

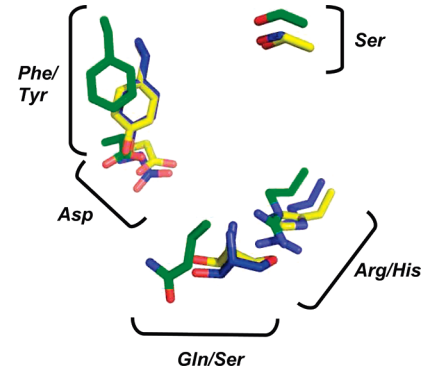

FIGURE 6: Superposition of residues forming a subsite in the active site of *E. coli* PBP4, *Actinomadura* R39 DD-peptidase, and *B. subtilis* PBP4a. Stick representation showing the side chains of residues in the *E. coli* PBP4 (green, PDB 2EX2), *B. subtilis* PBP4a (yellow, PDB 2J9P), and *Actinomadura* R39 DD-peptidase (blue, PDB 1W79) active sites important in substrate specificity. The active site serine is also shown; nitrogens are shown in blue and oxygens in red.

diacetyl-L-lysyl-D-alanyl-D-alanine (*33*). The available kinetic and structural data led us to speculate that a subsite in PBP4 may have a role in mediating substrate specificity, which is confirmed by our analysis of site-directed mutants showing Asp155, Arg361, and Gln422 are all important in PBP4-catalyzed DD-carboxypeptidation.

Questions still remain regarding class C LMM-PBPs and why certain enzymes (*Actinomadura* R39 DD-peptidase and *E. coli* PBP4) display a strong preference for the third residue of the stem peptide and others (*B. subtilis* PBP4a and *N. gonorrhoeae* PBP3) seemingly do not. The elegant structural data presented in refs *17* and *19* and kinetics and mutagenesis presented here provide compelling evidence that this substrate specificity is due in large part to residues forming a subsite or pocket in the active site of *Actinomadura* R39 DD-peptidase and *E. coli* PBP4. Superposition of the residues forming the subsite (Figure 6) shows their position to be highly conserved, and the X-ray crystal structure of *B. subtilis* PBP4a with a covalently attached peptidoglycan-mimetic shows interactions with the subsite. However, this enzyme demonstrates only moderate activity compared to both

Actinomadura R39 DD-peptidase and *E. coli* PBP4 with a monomer muropeptide substrate (*17*). The ϵ-carboxylate of *meso*-2,6-diaminopimelic acid in *B. subtilis* peptidoglycan is amidated, and it is probable that the K_m for an amidated peptide would be markedly lower; additionally, PBP4a may have a preference for a polymeric substrate such as a muropeptide dimer (*30*). A more confusing problem is the exceptionally high rate of DD-carboxypeptidation catalyzed by *N. gonorrhoeae* PBP3, which does not seem to require a defined stem peptide composition for activity (*21*). The genome of *N. gonorrhoeae* encodes only four PBPs, so PBP3 may have evolved to accept a wide variety of substrates. However, the structural basis for this activity is not clarified by our data and remains to be elucidated. Simple sequence alignment of class C LMM-PBPs shows functional similarity of the residues comprising the subsite, but the overall kinetic properties are clearly determined by additional features of individual enzymes.

Comparatively little attention has been given to characterizing the DD-endopeptidase activity of class C LMM-PBPs. The extended structure of the DD-endopeptidase substrate could result in different enzyme−substrate interactions, and therefore different features of the substrate or enzyme may be important for DD-carboxypeptidase activity compared to DD-endopeptidation. Mutation of the active site subsite affected DD-endopeptidation and again highlighted the importance of the amino acid residues involved in the recognition of the ϵ-carboxylate group of *meso*-2,6-diaminopimelic acid. The difference in structure between the substrates for DD-endopeptidation and DD-carboxypeptidation (polymeric versus monomeric) and the heterogeneity of the insoluble peptidoglycan preparation must be borne in mind when interpreting these results. For both monomeric and polymeric substrates, the ϵ-carboxylate is free and could thus form the same interactions with Arg361 and Gln422 that occur in DD-carboxypeptidation. However, free ϵ-ammonium groups are only present on the ends of the peptidoglycan polymers. It is possible that residues of the active site pocket (specifically Asp155) could still hydrogen bond with the −NH− of the cross-linking peptide bond, or the enzyme may display a preference for a free ϵ-ammonium group. This possible preference is hinted at by other *in vitro* DD-endopeptidase data (*34*), showing PBP4 preferentially cleaved short muropeptides and was less effective at cleaving muropeptide trimers and tetramers. Favorable interactions between the subsite and free ϵ-ammonium group of the *meso*-2,6-diaminopimelic acid present in a muropeptide dimer could be responsible for this preference.

Changes in DD-endopeptidase activity for all PBP4 mutants were minor in comparison to changes in DD-carboxypeptidase activity. For DD-carboxypeptidation, substitution of Asp155, Phe160, Arg361, and Gln422 primarily affected K_m, with only marginal changes in k_{cat}. Due to the low sensitivity of the turbidometric assay, a high concentration of peptidoglycan was used to follow DD-endopeptidation; it is possible that greater changes in DD-endopeptidase activity between mutants may be observed at lower, subsaturating, peptidoglycan concentrations. PBP4 may also engage in further (as yet) undefined interactions with other parts of the peptidoglycan polymer, in addition to those with Asp155, Arg361, and Gln422, that could also influence DD-endopeptidase activity. There is increasing *in vitro* and *in vivo* data indicating PBPs operate in multiprotein complexes with other PBPs and cell wall modifying enzymes (*28*); therefore, PBP4 DD-endopeptidase activity may be higher in a multiprotein milieu due to the formation of an extended substrate binding site with other proteins and preferential substrate positioning. However, the high DD-carboxypeptidase activity of PBP4 *in vitro* and the loose association of class C LMM-PBPs with the plasma membrane mean the importance of supplementary proteins for PBP4 activity requires further study.

The current understanding of *E. coli* PBP4 suggests that its optimal substrate is either a muropeptide monomer or dimer. PBP7, the other penicillin-sensitive DD-endopeptidase, accepts only high molecular mass murein sacculi as substrates *in vitro* (*35*), which implies a possible difference in the function of these two enzymes. It has been proposed that PBP7 is only involved in modifying peptidoglycan during cell division (*35*), whereas PBP4 can cleave smaller muropeptides and may function in peptidoglycan recycling. It is probable that there is a degree of redundancy in the roles of PBP4 and PBP7; however, further work *in vivo* and *in vitro* is required to delineate the exact functions of the LMM-PBPs in the metabolism of *E. coli* peptidoglycan. An additional complicating factor in ascribing a specific role to PBP4 is that the *E. coli* genome encodes another DD-endopeptidase (MepA) (*36*), a penicillin-insensitive enzyme which has been shown to cleave muropeptide dimers and insoluble murein sacculi *in vitro* (*36, 37*). The functional overlap between PBP4 and MepA *in vivo* is unknown as studies on *E. coli* strains with defined PBP deletion mutations did not include the *mepA* gene (*11*).

Recognition of the third position residue of the stem peptide by *E. coli* PBP4 may be a reflection of the differing substrate requirements of bifunctional DD-carboxypeptidase/DD-endopeptidases compared to monofunctional DD-carboxypeptidases or DD-transpeptidases. It has been proposed (*19*) that the lack of recognition of extended features of peptidoglycan by HMM-PBPs and class A LMM-PBPs is a defense mechanism to counter potential inhibition. The presence of elements for the recognition of such features may be limited to class C LMM-PBPs as it is a strict requirement for efficient enzyme activity, even at the expense of potential inhibition.

ACKNOWLEDGMENT

We thank Hiroyuki Kishida (Yokohama City University, Japan) for *dacB* expression constructs and technical assistance and also Prof. R. C. Levesque (Université Laval, Canada) and Dr. A. M. Blewett (University of Warwick, U.K.) for providing Mur enzyme expression constructs used for substrate synthesis. Additionally, we thank Dr. G. De Pascale (McMaster University, Canada) for assistance with substrate preparation.

SUPPORTING INFORMATION AVAILABLE

Far-UV circular dichroism spectra of wild-type and *E. coli* PBP4 mutants confirming site-directed mutagenesis had not disrupted the structure of PBP4. This material is available free of charge via the Internet at http://pubs.acs.org.

REFERENCES

1. Vollmer, W., Blanot, D., and de Pedro, M. A. (2008) Peptidoglycan structure and architecture. *FEMS Microbiol. Rev. 32*, 149–167.

2. Vollmer, W., and Bertsche, U. (2008) Murein (peptidoglycan) structure, architecture and biosynthesis in *Escherichia coli*. *Biochim. Biophys. Acta 1778*, 1714–1734.
3. Schleifer, K. H., and Kandler, O. (1972) Peptidoglycan types of bacterial cell walls and their taxonomic implications. *Bacteriol. Rev. 36*, 407–477.
4. Sauvage, E., Kerff, F., Terrak, M., Ayala, J. A., and Charlier, P. (2008) The penicillin-binding proteins: structure and role in peptidoglycan biosynthesis. *FEMS Microbiol. Rev. 32*, 234–258.
5. Goffin, C., and Ghuysen, J. M. (1998) Multimodular penicillin-binding proteins: an enigmatic family of orthologs and paralogs. *Microbiol. Mol. Biol. Rev. 62*, 1079–1093.
6. Popham, D. L., and Young, K. D. (2003) Role of penicillin-binding proteins in bacterial cell morphogenesis. *Curr. Opin. Microbiol. 6*, 594–599.
7. Massova, I., and Mobashery, S. (1998) Kinship and diversification of bacterial penicillin-binding proteins and beta-lactamases. *Antimicrob. Agents Chemother. 42*, 1–17.
8. Ghosh, A. S., Chowdhury, C., and Nelson, D. E. (2008) Physiological functions of D-alanine carboxypeptidases in *Escherichia coli*. *Trends Microbiol. 16*, 309–317.
9. Silvaggi, N. R., Josephine, H. R., Kuzin, A. P., Nagarajan, R., Pratt, R. F., and Kelly, J. A. (2005) Crystal structures of complexes between the R61 DD-peptidase and peptidoglycan-mimetic beta-lactams: a non-covalent complex with a "perfect penicillin". *J. Mol. Biol. 345*, 521–533.
10. Korat, B., Mottl, H., and Keck, W. (1991) Penicillin-binding protein 4 of *Escherichia coli*: molecular cloning of the dacB gene, controlled overexpression, and alterations in murein composition. *Mol. Microbiol. 5*, 675–684.
11. Denome, S. A., Elf, P. K., Henderson, T. A., Nelson, D. E., and Young, K. D. (1999) *Escherichia coli* mutants lacking all possible combinations of eight penicillin binding proteins: viability, characteristics, and implications for peptidoglycan synthesis. *J. Bacteriol. 181*, 3981–3993.
12. Holtje, J. V. (1998) Growth of the stress-bearing and shape-maintaining murein sacculus of *Escherichia coli*. *Microbiol. Mol. Biol. Rev. 62*, 181–203.
13. Spratt, B. G. (1977) Properties of the penicillin-binding proteins of *Escherichia coli* K12. *Eur. J. Biochem. 72*, 341–352.
14. Nelson, D. E., and Young, K. D. (2001) Contributions of PBP 5 and DD-carboxypeptidase penicillin binding proteins to maintenance of cell shape in *Escherichia coli*. *J. Bacteriol. 183*, 3055–3064.
15. Kishida, H., Unzai, S., Roper, D. I., Lloyd, A., Park, S. Y., and Tame, J. R. (2006) Crystal structure of penicillin binding protein 4 (dacB) from *Escherichia coli*, both in the native form and covalently linked to various antibiotics. *Biochemistry 45*, 783–792.
16. Nicholas, R. A., Krings, S., Tomberg, J., Nicola, G., and Davies, C. (2003) Crystal structure of wild-type penicillin-binding protein 5 from *Escherichia coli*: implications for deacylation of the acyl-enzyme complex. *J. Biol. Chem. 278*, 52826–52833.
17. Sauvage, E., Duez, C., Herman, R., Kerff, F., Petrella, S., Anderson, J. W., Adediran, S. A., Pratt, R. F., Frere, J. M., and Charlier, P. (2007) Crystal structure of the *Bacillus subtilis* penicillin-binding protein 4a, and its complex with a peptidoglycan mimetic peptide. *J. Mol. Biol. 371*, 528–539.
18. Sauvage, E., Herman, R., Petrella, S., Duez, C., Bouillenne, F., Frere, J. M., and Charlier, P. (2005) Crystal structure of the Actinomadura R39 DD-peptidase reveals new domains in penicillin-binding proteins. *J. Biol. Chem. 280*, 31249–31256.
19. Sauvage, E., Powell, A. J., Heilemann, J., Josephine, H. R., Charlier, P., Davies, C., and Pratt, R. F. (2008) Crystal structures of complexes of bacterial DD-peptidases with peptidoglycan-mimetic ligands: the substrate specificity puzzle. *J. Mol. Biol. 381*, 383–393.
20. Anderson, J. W., Adediran, S. A., Charlier, P., Nguyen-Disteche, M., Frere, J. M., Nicholas, R. A., and Pratt, R. F. (2003) On the substrate specificity of bacterial DD-peptidases: evidence from two series of peptidoglycan-mimetic peptides. *Biochem. J. 373*, 949–955.
21. Stefanova, M. E., Tomberg, J., Olesky, M., Holtje, J. V., Gutheil, W. G., and Nicholas, R. A. (2003) *Neisseria gonorrhoeae* penicillin-binding protein 3 exhibits exceptionally high carboxypeptidase and beta-lactam binding activities. *Biochemistry 42*, 14614–14625.
22. Liu, H., Sadamoto, R., Sears, P. S., and Wong, C. H. (2001) An efficient chemoenzymatic strategy for the synthesis of wild-type and vancomycin-resistant bacterial cell-wall precursors: UDP-N-acetylmuramyl-peptides. *J. Am. Chem. Soc. 123*, 9916–9917.
23. Lloyd, A. J., Gilbey, A. M., Blewett, A. M., De Pascale, G., El Zoeiby, A., Levesque, R. C., Catherwood, A. C., Tomasz, A., Bugg, T. D., Roper, D. I., and Dowson, C. G. (2008) Characterization of tRNA-dependent peptide bond formation by MurM in the synthesis of *Streptococcus pneumoniae* peptidoglycan. *J. Biol. Chem. 283*, 6402–6417.
24. Gutheil, W. G., Stefanova, M. E., and Nicholas, R. A. (2000) Fluorescent coupled enzyme assays for D-alanine: application to penicillin-binding protein and vancomycin activity assays. *Anal. Biochem. 287*, 196–202.
25. Bernadsky, G., Beveridge, T. J., and Clarke, A. J. (1994) Analysis of the sodium dodecyl sulfate-stable peptidoglycan autolysins of select gram-negative pathogens by using renaturing polyacrylamide gel electrophoresis. *J. Bacteriol. 176*, 5225–5232.
26. Hash, J. H. (1967) Measurement of bacteriolytic enzymes. *J. Bacteriol. 93*, 1201–1202.
27. Cheng, X., Zhang, X., Pflugrath, J. W., and Studier, F. W. (1994) The structure of bacteriophage T7 lysozyme, a zinc amidase and an inhibitor of T7 RNA polymerase. *Proc. Natl. Acad. Sci. U.S.A. 91*, 4034–4038.
28. Josephine, H. R., Charlier, P., Davies, C., Nicholas, R. A., and Pratt, R. F. (2006) Reactivity of penicillin-binding proteins with peptidoglycan-mimetic beta-lactams: what's wrong with these enzymes? *Biochemistry 45*, 15873–15883.
29. Hesek, D., Suvorov, M., Morio, K., Lee, M., Brown, S., Vakulenko, S. B., and Mobashery, S. (2004) Synthetic peptidoglycan substrates for penicillin-binding protein 5 of Gram-negative bacteria. *J. Org. Chem. 69*, 778–784.
30. Pratt, R. F. (2008) Substrate specificity of bacterial DD-peptidases (penicillin-binding proteins). *Cell. Mol. Life Sci. 65*, 2138–2155.
31. Anderson, J. W., and Pratt, R. F. (2000) Dipeptide binding to the extended active site of the *Streptomyces* R61 D-alanyl-D-alanine-peptidase: the path to a specific substrate. *Biochemistry 39*, 12200–12209.
32. McDonough, M. A., Anderson, J. W., Silvaggi, N. R., Pratt, R. F., Knox, J. R., and Kelly, J. A. (2002) Structures of two kinetic intermediates reveal species specificity of penicillin-binding proteins. *J. Mol. Biol. 322*, 111–122.
33. Stefanova, M. E., Davies, C., Nicholas, R. A., and Gutheil, W. G. (2002) pH, inhibitor, and substrate specificity studies on *Escherichia coli* penicillin-binding protein 5. *Biochim. Biophys. Acta 1597*, 292–300.
34. Li, S. Y., Holtje, J. V., and Young, K. D. (2004) Comparison of high-performance liquid chromatography and fluorophore-assisted carbohydrate electrophoresis methods for analyzing peptidoglycan composition of *Escherichia coli*. *Anal. Biochem. 326*, 1–12.
35. Romeis, T., and Holtje, J. V. (1994) Penicillin-binding protein 7/8 of *Escherichia coli* is a DD-endopeptidase. *Eur. J. Biochem. 224*, 597–604.
36. Marcyjaniak, M., Odintsov, S. G., Sabala, I., and Bochtler, M. (2004) Peptidoglycan amidase MepA is a LAS metallopeptidase. *J. Biol. Chem. 279*, 43982–43989.
37. Firczuk, M., and Bochtler, M. (2007) Mutational analysis of peptidoglycan amidase MepA. *Biochemistry 46*, 120–128.

BI801993X